

Modal Reduction of a Nonlinear Rotating Beam Through Nonlinear Normal Modes*

Eric Pesheck

Mechanical Dynamics, Inc.,
Ann Arbor, MI 48105
email: epesh@adams.com

Christophe Pierre

Fellow ASME
Department of Mechanical Engineering,
University of Michigan,
Ann Arbor, MI 48109
email: pierre@umich.edu

Steven W. Shaw

Fellow ASME
Department of Mechanical Engineering,
Michigan State University,
East Lansing, MI 48824-1226
email: shaw@egr.msu.edu

A method for determining reduced-order models for rotating beams is presented. The approach is based on the construction of nonlinear normal modes that are defined in terms of invariant manifolds that exist for the system equations of motion. The beam considered is an idealized model for a rotor blade whose motions are dominated by transverse vibrations in the direction perpendicular to the plane of rotation (known as flapping). The mathematical model for the rotating beam is relatively simple, but contains the nonlinear coupling that exists between transverse and axial deflections. When one employs standard modal expansion or finite element techniques to this system, this nonlinearity causes slow convergence, leading to models that require many degrees of freedom in order to achieve accurate dynamical representations. In contrast, the invariant manifold approach systematically accounts for the nonlinear coupling between linear modes, thereby providing models with very few degrees of freedom that accurately capture the essential dynamics of the system. Models with one and two nonlinear modes are considered, the latter being able to handle systems with internal resonances. Simulation results are used to demonstrate the validity of the approach and to exhibit features of the nonlinear modal responses. [DOI: 10.1115/1.1426071]

Introduction

The determination of rotorcraft blade dynamics has been the subject of considerable study. These dynamics are difficult to obtain accurately, since the rotation, together with the blade geometry, produces significant nonlinear effects. These effects arise from transverse/axial coupling through the axial strain, and result in slow convergence when the system is analyzed using modal expansion approaches or finite element techniques. Hence, many degrees of freedom (DOF) are required to obtain an accurate dynamic model.

Much work has been done to create nonlinear finite element schemes which are capable of accurate analysis [1–3]. However, this approach yields large models which often render complete nonlinear analysis impractical. Consequently, it is typical to use the full model to determine the nonlinear equilibrium solution, and then linearize about this solution. This approach ignores many nonlinear dynamic terms, and may predict inaccurate results.

Alternatively, several general analytic formulations have been developed [4–6]. These formulations, though applicable for a wide variety of parameters and blade geometries, are difficult to use, as they are quite complex. Ultimately, this approach yields equations which are no more transparent than those from the finite element approach.

Consequently, many studies of these systems are done on highly idealized models [7–10], as results are more easily obtained, and new strategies and methods may be evaluated more effectively. The nonlinearities obtained in such cases are more manageable, and the qualitative behavior may often be extrapolated to more realistic systems.

In this study, such an idealized model is used. We consider a uniform cantilevered Euler-Bernoulli beam, rotating at constant velocity, and constrained to deform in the transverse (flapping) and axial directions. The resulting equations are discretized using the linear modes of the rotating beam, and nonlinearities in slope and displacement are retained through third order, yielding a set of

modal equations which are linearly uncoupled, but coupled at quadratic and cubic order. The modal convergence of this system is then evaluated to ensure a reference model of sufficient accuracy.

This model is then reduced using several different approaches, including the use of multi-mode invariant manifolds [11], a direct extension of the manifold-based nonlinear normal modes (NNM's) first developed by Shaw and Pierre [12,13]. This approach results in reduced-order models which include the most prominent effects of all nonmodeled linear modes, while allowing arbitrary sets of modes to be chosen as the modeled subset. These reduced models are efficient, and formulated such that they may easily be extended to considerably more complex rotor blade models—both analytic and finite-element based.

The results indicate that, though the transverse dynamics are of primary interest, it is necessary to account for the influence of extensional motions. The NNM-based reduction procedure embeds all nonlinear interactions between linear modes, including the crucial axial-transverse coupling, without requiring the explicit simulation necessitated by the traditional (linear modal analysis) approach. Consequently, the NNM-based reduced models are considerably more accurate than other models of equivalent size.

Formulation

The uniform rotating Euler-Bernoulli beam shown in Fig. 1 is considered. We neglect rotatory inertia, restrict motion to a rotating plane (thus eliminating lead-lag and torsional motions), and allow nonlinear axial strain. This strain is the source of the axial/transverse coupling that leads to modal convergence problems for this system. Note that other nonlinear effects, such as those due to curvature, are not included since they do not play a crucial role in convergence issues. Hence, the potential energy, U , and kinetic energy, T , may be expressed as follows:

$$T = \frac{1}{2} \int_0^L m(\dot{u}^2 + \dot{w}^2) + m\Omega^2(h + x + u)^2 dx \quad (1)$$

*Paper also was presented at DETC-99, Las Vegas, NV

Contributed by the Technical Committee on Vibration and Sound for publication in the JOURNAL OF VIBRATION AND ACOUSTICS. Manuscript received Nov. 1999; Revised Aug. 2001. Associate Editor: A. F. Vakakis.

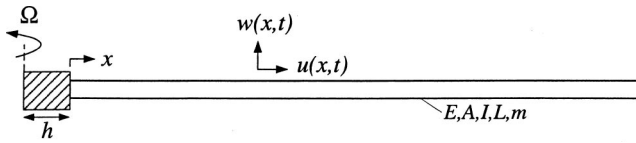


Fig. 1 Rotating beam system, $\Omega=\text{constant}$

$$U = \frac{1}{2} \int_0^L EI(w_{,xx})^2 + EA \left(u_{,x} + \frac{1}{2} (w_{,x})^2 \right)^2 dx \quad (2)$$

where $u(x,t)$ and $w(x,t)$ are the axial and transverse displacements respectively, $(\cdot)_{,x}$ is a derivative with respect to the spatial variable x , an overdot represents a time derivative, h is the hub radius, Ω is the constant angular velocity of the beam, m is the beam mass per unit length, and $E, A, I,$ and L are the typical beam parameters. These expressions, and Hamilton's principle, are used to develop the following weak formulation for the equations of motion:

$$\int_{t_1}^{t_2} \int_0^L \left\{ \left[-m\ddot{w}\delta w - EIw_{,xx}\delta w_{,xx} - EA \left(u_{,x} + \frac{1}{2} (w_{,x})^2 \right) w_{,x} \delta w_{,x} \right] \right. \\ \left. + \left[-m\ddot{u}\delta u + m\Omega^2(x+h+u)\delta u \right] \right. \\ \left. - EA \left(u_{,x} + \frac{1}{2} (w_{,x})^2 \right) \delta u_{,x} \right\} dx dt = 0 \quad (3)$$

where $\delta(\cdot)$ denotes the variation of a quantity.

With the foreknowledge that these equations will be discretized using the fixed-free axial bar modes and fixed-free transverse modes of the nonrotating linear beam (and their corresponding boundary conditions), these expressions are reduced through integration by parts to:

$$\int_{t_1}^{t_2} \int_0^L \left\{ \left[-m\ddot{w} - EIw_{,xxxx} \right] \delta w - \left[EA \left(u_{,x} + \frac{1}{2} (w_{,x})^2 \right) w_{,x} \right] \delta w_{,x} \right. \\ \left. + \left[-m\ddot{u} + m\Omega^2(x+h+u) + EAu_{,xx} \right] \delta u \right. \\ \left. - \left[EA \frac{1}{2} (w_{,x})^2 \right] \delta u_{,x} \right\} dx dt = 0 \quad (4)$$

At this point it is convenient to separate $u(x,t)$ into static and dynamic components, as follows:

$$u(x,t) = u_s(x) + u_d(x,t) \quad (5)$$

where $u_s(x)$ satisfies the static version of the equations with $w(x,t) \equiv 0$, given by

$$u_{s,xx} + \lambda^2 u_s = -\lambda^2 (h+x),$$

where $\lambda^2 = m\Omega^2/EA$. Using the appropriate boundary conditions, it is found that

$$u_s(x) = \frac{1 + \lambda h \sin(\lambda L)}{\lambda \cos(\lambda L)} \sin(\lambda x) + h \cos(\lambda x) - (h+x)$$

which represents the static elongation of the beam due to rotation when it has zero transverse deflection. When Eq. (5) is substituted into Eq. (4) and the nonlinear terms are neglected (for now), we are left with two linear partial differential equations for the rotating beam, whose modal solutions will decouple the fully nonlinear equations of motion to linear order. These are:

$$m\ddot{u}_d - m\Omega^2 u_d - EAu_{d,xx} = 0 \quad (6)$$

$$m\ddot{w} + EIw_{,xxxx} - EA(u_{s,x}w_{,xx} + u_{s,xx}w_{,x}) = 0. \quad (7)$$

In the axial direction, the mode shapes of the rotating beam, $\phi_i(x)$, are the same as the well known axial mode shapes for a

uniform (fixed-free) nonrotating beam. However, the transverse mode shapes of the rotating beam, $\psi_i(x)$, can be approximated using a Rayleigh-Ritz procedure [14], as:

$$\psi_i(x) = \sum_{j=1}^{N_c} \eta_{ij} \theta_j(x)$$

where the $\theta_j(x)$ are the familiar modes of a (nonrotating) fixed-free beam. Once the modes of the linearized rotating beam are determined, modal solutions to the nonlinear equations are sought in the form:

$$u_d = \sum_{i=1}^{N_a} a_i(t) \phi_i(x) \quad w = \sum_{i=1}^{N_t} c_i(t) \psi_i(x). \quad (8)$$

The integers $N_a, N_t,$ and N_c are used to denote the number of modes included in each of the above expansions.

These discretizations are substituted into the weak formulation, Eq. (4), the result is projected onto the linear modes, and orthogonality is invoked, resulting in the following discretized nonlinear equations of motion:

$$\ddot{a}_j + (\omega_{a,j})^2 a_j + \frac{EA}{2} \sum_{k=1}^{N_t} \sum_{l=k}^{N_t} c_k c_l \int_0^L \gamma(k,l,x) \phi_{j,x} dx = 0 \\ \text{for } j=1 \dots N_a \quad (9)$$

$$\ddot{c}_j + (\omega_{t,j})^2 c_j + EA \left[\sum_{k=1}^{N_a} \sum_{l=1}^{N_t} a_k c_l \int_0^L \phi_{k,x} \psi_{l,x} \psi_{j,x} dx \right. \\ \left. + \frac{1}{2} \sum_{k=1}^{N_t} \sum_{l=k}^{N_t} \sum_{i=l}^{N_t} c_k c_l c_i \int_0^L \sigma(k,l,i,x) \psi_{j,x} dx \right] = 0 \\ \text{for } j=1 \dots N_t, \quad (10)$$

where γ and σ are defined as

$$\gamma(i,j,x) = \begin{cases} \psi_{i,x}^2 & i=j \\ 2\psi_{i,x}\psi_{j,x} & i \neq j \end{cases} \quad (11)$$

$$\sigma(k,l,i,x) = \begin{cases} \psi_{k,x}^3 & k=l=i \\ 3\psi_{k,x}^2\psi_{i,x} & k=l \neq i \\ 3\psi_{l,x}^2\psi_{k,x} & k \neq l=i \\ 6\psi_{k,x}\psi_{l,x}\psi_{i,x} & k \neq l \neq i \end{cases} \quad (12)$$

and $\omega_{a,j}$ and $\omega_{t,j}$ are the natural frequencies associated with the j th modes in the axial and transverse directions, respectively. The transverse natural frequencies, $\omega_{t,j}$, were compared against those in [7] and found to be in good agreement. Small differences ($\approx .05$ percent) were traced to different extensibility assumptions. Note that the nonlinearities dictate a particular form of nonlinear coupling between the two sets of differential equations. It is this nonlinear interaction which produces axial shortening as a consequence of transverse bending, as well as the cubic stiffening due to nonlinear strains.

Often, in systems such as this, quasi-static assumptions are employed. In this case, the accelerations in the axial direction, $[\ddot{a}_j]$ in Eq. (9)], are neglected, allowing each a_j to be determined as a quadratic function of the c_k 's. These expressions are then inserted into Eq. (10) to achieve a system model with purely cubic system, which governs the dynamics in the transverse direction. Though some results are shown in which this approach was used, it is not emphasized here, since more complete rotorcraft system models contain coupling terms and inertial effects which cannot be accounted for by using quasi-static assumptions.

The accuracy of this reduced system of equations depends primarily upon three parameters: N_c , the number of component (nonrotating fixed-free beam) modes used to assemble each transverse rotating mode; N_t , the number of transverse rotating modes used for $w(x,t)$; and N_a , the number of axial modes used for

Table 1 The first several transverse and axial natural frequencies (in rad/s) both at rest ($\Omega=0$) and at the nominal rotation rate ($\Omega=30$ rad/s)

	$\omega_{t,1}$	$\omega_{t,2}$	$\omega_{t,3}$	$\omega_{t,4}$	$\omega_{a,1}$	$\omega_{a,2}$
$\Omega = 0$	8.672	54.35	152.2	298.2	824.7	2474.0
$\Omega = 30$	34.03	95.84	200.5	351.5	824.1	2473.9

$u_d(x,t)$. In order to effectively evaluate the proposed model reduction methods, it is necessary to obtain an accurate discretized reference model. As such, the convergence of the system properties and dynamics must be investigated in order to determine acceptable values for N_c , N_t , and N_a .

System Convergence

Several properties of the system may be evaluated as the numbers of included modes are varied, and the convergence of these properties will be used here as a general guide in determining a minimal model size for accurate results. In this study, the primary focus is on the dynamics of the lower frequency transverse modes of an approximate helicopter rotor blade model. The nominal parameters used to study the system convergence are as follows: $L = 9$ m, $m = 10$ kg/m, $EI = 3.99 \times 10^5$ N·m², $EA = 2.23 \times 10^8$ N, $\Omega = 30$ rad/s, and $h = 0.5$ m. It is assumed that reasonable deviations from these parameters will have little effect on the system convergence. For the reader's reference, the first several transverse and axial natural frequencies are shown in Table 1, using the nominal parameters above, with rotation rates of $\Omega=0$ and $\Omega=30$ rad/s (nearly transonic blade tip velocity). Note that the axial modes, as expected, have much higher natural frequencies, and this is the motivation for the quasi-static approximation that is frequently employed.

It is necessary to investigate the convergence behavior relative to N_c (the number of stationary transverse component modes) first, as this will dictate both the accuracy of the transverse modes, and the system dynamics as a whole. This convergence may be evaluated through examination of the properties of the assembled rotating modes of the system for various values of N_c . The assembled mode shapes $\psi_j(x)$ converge quite quickly, showing very little difference for $N_c > 4$. However, the associated rotating beam natural frequencies ($\omega_{t,j}$) converge considerably slower. It has been found that for $N_c = 11$ the first three natural frequencies are correct through four decimal places. For higher modes, the effects of the beam rotation are less prominent, and the $\psi_j(x)$ approach the corresponding nonrotating component modes, $\theta_j(x)$. Therefore, higher transverse modes ($j > 10$) may be well approximated by only including several component modes above and below j . Based on these results, it was decided to use the empirical formula: $N_c = N_t + 9$ to determine N_c . Again, this guideline is tailored to the model parameters and modes of interest considered here.

Next, the effects of N_a , the number of axial modes, are evaluated. This is done two ways: First, through examination of the

axial deformation, $u_d(x)$, due to a static transverse deflection, $w(x)$. Second, through numerical integration of the discretized equations of motion, Eqs. (9) and (10), for a fixed N_t , and various values of N_a .

Figure 2 depicts a particular static transverse deflection, $w(x)$, and the attendant axial deformation for various values of N_a . These results are produced by choosing a deformation, $w(x)$, determining the corresponding c_j 's, substituting them into Eq. (9), assuming a static solution, solving for the N_a a_j 's, and reconstructing the final axial deformation shape. This illustrates the ability of the axial deformation to react properly to deformations in the transverse direction. In Fig. 2, $w(x)$ is the second transverse linear mode, $\psi_2(x)$, and it is easily seen that the convergence of $u_x(x)$ is quite slow, requiring at least six axial modes to capture the general character of the deformation. It should be noted that convergence near $x=L$ will be particularly slow, due to the choice of axial modal functions, $\phi_j(x)$, which do not satisfy the actual boundary conditions at the blade tip. However, this error is confined to the beam tip, and as such, its effects on the overall system are expected to be small.

Since the dynamics in the transverse direction are of primary interest, it is worthwhile to examine directly the transverse motions and the resulting axial deflections for various values of N_a . Figures 3 and 4 depict the dynamics of the beam tip in the transverse and axial directions, respectively, for $N_a = 1, 3, 6,$ and 9 , with an initial deflection in the second transverse linear mode. All simulations are carried out using a fourth order Runge-Kutta integration scheme, and six transverse (rotating) modes ($N_t = 6$). The results indicate that the primary effects of N_a on the transverse dynamics, $w(x,t)$, are in the response frequency, with secondary effects in amplitude. It may be seen that the transverse dynamics are well captured by six axial modes, although nine axial modes yield an additional frequency correction. Figure 4 highlights the nonlinear dynamics in the axial direction. Here, the dynamic participation of the additional axial modes is apparent, since the inclusion of more axial modes clearly produces higher frequency components in the response. It should be noticed that Figs. 3 and 4 show considerably different time frames, with approximately one period of the oscillations of Fig. 3 apparent as a slow harmonic component of Fig. 4. The high frequency dynamics visible in Fig. 4 are largely a result of the "ringing" of the axial modes due to nonlinear internal stresses which result from the initial conditions. That is, the initial conditions assume deflections in $w(x)$ only, without the corresponding (equilibrium producing) deflections in $u(x)$. However, the high frequency content of these dynamics aids in the accurate evaluation of model convergence. Once again, small differences are observed between the dynamics produced using six and nine axial modes. Hence nine axial modes ($N_a = 9$) are used for the final system model.

Next, it is necessary to determine the number of transverse rotating modes, N_t , to be used. As with the axial modes, this is done by comparing the dynamic beam response for various values of N_t . Figure 5 shows the transverse response at the beam tip, $w(L,t)$, for an initial condition in the second transverse linear

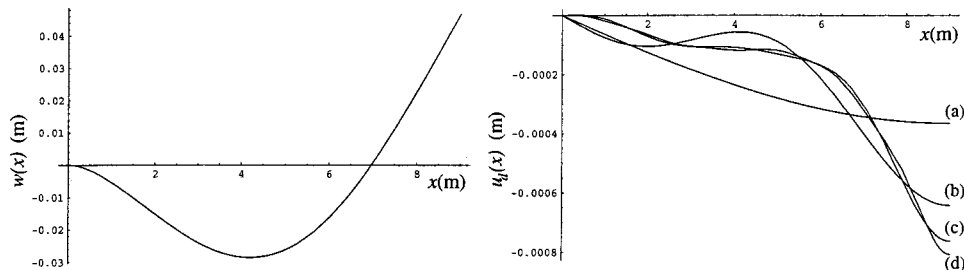


Fig. 2 Axial deflection, $u_d(x)$, due to a static transverse deflection, $w(x)$, for various values of N_a ; (a) $N_a=1$, (b) $N_a=3$, (c) $N_a=6$, (d) $N_a=12$

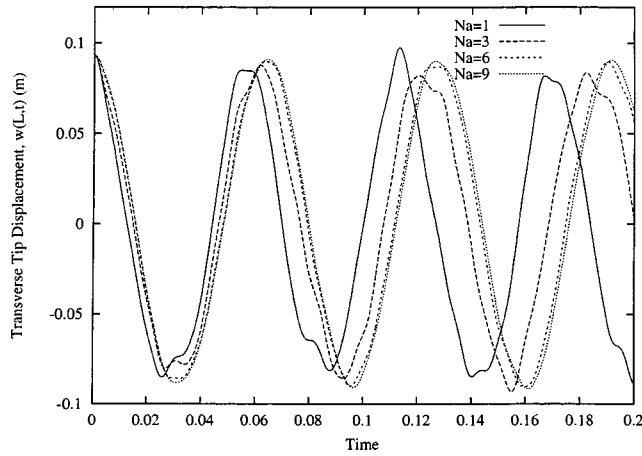


Fig. 3 Transverse dynamics initiated in the second transverse linear mode, shown at the beam tip, for various values of N_a

mode, with $N_t=3, 6,$ and 9 . The latter two responses are quite close, but as small differences may still be observed between $N_t=6$ and $N_t=9$, and since the transverse dynamics are of greatest interest, the higher value was chosen.

Through these procedures, the final model was chosen to contain $N_c=18$ stationary fixed-free beam modes, which are used to generate $N_t=9$ transverse rotating modes. These transverse modes are then coupled to $N_a=9$ axial modes, for a final model size of $N=N_t+N_a=18$ modes. It is recognized that, due to the limited nature of this convergence study, and the well documented convergence difficulties for similar rotating systems, this model is somewhat minimal. However, it is of sufficient size to effectively demonstrate the nonlinear normal mode-based reduction procedure, and it will henceforth be referred to as the *reference model*.

An additional check of this model is illustrated in Fig. 6, which shows the periodic response frequency of the first nonlinear mode as a function of the number of total model linear modes for a given motion amplitude. For this example, equal numbers of axial and transverse linear modes were used, so the abscissa corresponds to N_a+N_t . One can see that, at this amplitude, the nonlinear response frequency is accurately determined by an 18 mode model. The periodic solutions used for this figure were obtained computationally by locating initial conditions in the vicinity of the

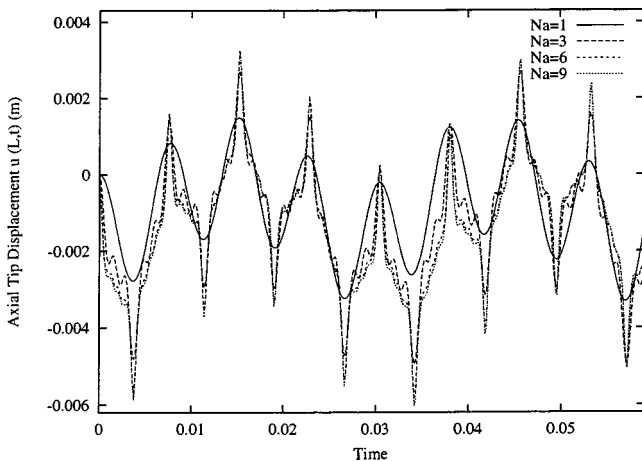


Fig. 4 Axial dynamics due to initial conditions in the second linear transverse mode, shown at the beam tip, for various values of N_a

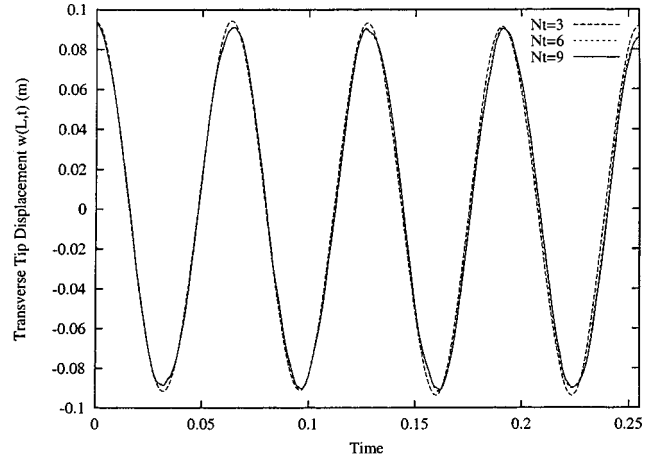


Fig. 5 Transverse dynamics initiated in the second transverse linear mode, shown at the beam tip, for various values of N_t

first NNM which yield a periodic solution. These solutions will, in fact, lie on the invariant manifold which is the basis of our reduction technique.

Nonlinear Mode-Based Model Reduction

The approach used here to generate reduced order models of Eqs. (9) and (10) was originally developed by Shaw and Pierre [12]. It utilizes invariant manifolds in the system's phase space to generate constraint equations which dynamically "enslave" non-essential linear modal degrees of those of interest. The resulting reduced equations of motion capture many of the nonlinear influences of the enslaved DOF's without requiring explicit simulation of them. A general exposition of the procedure and systematic implementation used here may be found in [15]. The general formulation allows for the inclusion of damping, but the results for conservative systems, such as the one under consideration, simplify to those described herein.

For this system, the transverse motions are of primary interest. Therefore, one or more of the transverse modal coordinate pairs $((c, \dot{c})$'s), along with any internally resonant modal coordinates will be chosen as "master" coordinates, and the remaining coordinates will be enslaved. The set of "master" modal positions and

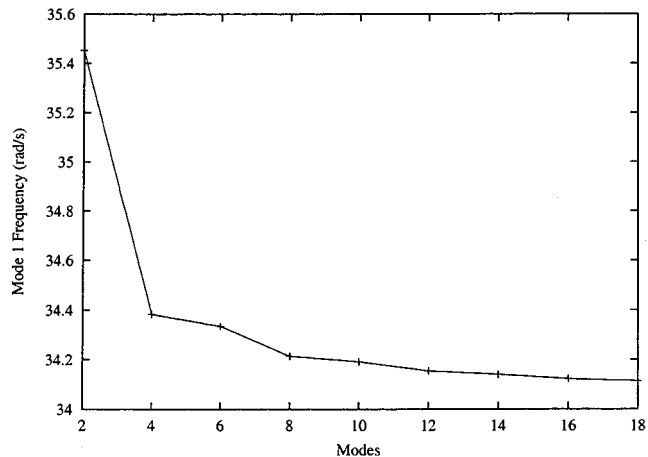


Fig. 6 First NNM frequency versus number of linear modes. Here, $N_a=N_t$, and $c_1(0)=1.0$, corresponding to an end deflection of $w(L)\approx 0.2$ m

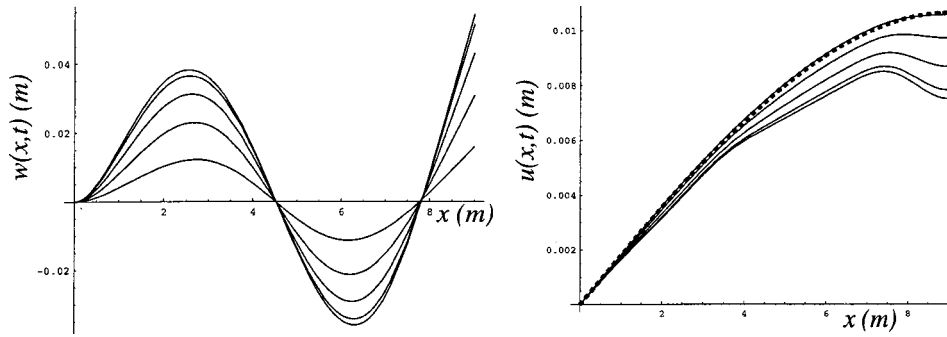


Fig. 7 Transverse and axial deflections, $w(x,t)$ and $u(x,t)$, for a quarter-period of motion in the third nonlinear mode. The deflections are shown at a set of equal time intervals spaced throughout the first quarter-period of the response. The dashed line denotes the static deflection, $u_s(x)$, and the top curve for $w(x)$ corresponds to the bottom $u(x)$ curve, which occur at $t=0$. Note that the beam starts with the maximum transverse deflection and the lowest axial deflection, and transitions to zero transverse deflection and $u(x,t) \approx u_s(x)$ at the quarter-period.

velocities is denoted by $(\mathbf{u}_M, \mathbf{v}_M)$, and the reduced differential equation(s) for the chosen transverse mode(s) is (are) of the following form:

$$\ddot{c}_j + \omega_{t,j}^2 c_j + f_{nl,j}(\mathbf{u}_M, \mathbf{v}_M) = 0 \quad \text{where } c_j \in \mathbf{u}_M \quad \text{and} \quad \dot{c}_j \in \mathbf{v}_M \quad (13)$$

The associated constraint equations are of the form:

$$\begin{aligned} c_k &= X_{t,k}(\mathbf{u}_M, \mathbf{v}_M) & \dot{c}_k &= Y_{t,k}(\mathbf{u}_M, \mathbf{v}_M) \\ \text{where } k &= 1 \dots N_t, c_k \in \mathbf{u}_M, \dot{c}_k \in \mathbf{v}_M \\ a_k &= X_{a,k}(\mathbf{u}_M, \mathbf{v}_M) & \dot{a}_k &= Y_{a,k}(\mathbf{u}_M, \mathbf{v}_M) \\ \text{where } k &= 1 \dots N_a, a_k \in \mathbf{u}_M, \dot{a}_k \in \mathbf{v}_M \end{aligned} \quad (14)$$

In this work we approximate the constraint equations (the X 's and Y 's) as third order polynomial expansions in the elements of $(\mathbf{u}_M, \mathbf{v}_M)$. The key to choosing these constraints in a systematic, dynamically relevant manner is that they are forced to satisfy the equations of motion. At this level of expansion, the nonlinear functions $f_{nl,j}$, which depend on the properties of the original system, contain third and fifth order polynomial terms in the elements of $(\mathbf{u}_M, \mathbf{v}_M)$. As an illustration, if $(\mathbf{u}_M, \mathbf{v}_M)$ consists of only the position and velocity of the third transverse mode, (c_3, \dot{c}_3) , the resulting NNM-reduced differential equation is of the form:

$$\ddot{c}_3 + \omega_{t,3}^2 c_3 + A_1 c_3^3 + A_2 c_3 \dot{c}_3^2 + A_3 c_3^5 + A_4 c_3^3 \dot{c}_3^2 + A_5 c_3 \dot{c}_3^4 = 0 \quad (15)$$

where the constants, A_i , are functions of the system parameters. Hence, only the coordinates in $(\mathbf{u}_M, \mathbf{v}_M)$ need to be simulated (using equations such as Eq. (13)), while the constraint equations are used to reconstruct the response of the enslaved linear modes. In the more general case there will be a set of master modes, resulting in a set of oscillators that are uncoupled at linear order and coupled through nonlinear terms. It is crucial to the method to realize that solutions of these equations of motion are also solutions of the original nonlinear equations of motion that describe the dynamics of the full model, that is, the one describing the dynamics of all the coupled linear modes. This is accomplished by capturing the invariant dynamics of the corresponding modes, which can be achieved from the full model only if one uses very special initial conditions and simulates all the modes accordingly.

This reduction procedure has been computationally automated for a certain class of nonlinear structural systems, which includes Eqs. (9) and (10), for which the coefficients of the nonlinear terms have been evaluated. One simply chooses the desired "master" coordinate set, and the reduced equations of motion and constraint equations are automatically generated. In cases of internal resonance, nonremovable coupling between resonant modes requires

augmenting the set of "master" modes to include all modes which are internally resonant with the original set. That is, internally resonant groups of modes must lie entirely in either the "master" or "slave" subgroups. More complete expositions of this material may be found in [11,15]

The rotating beam system is particularly well suited for this reduction procedure for two reasons. First, the axial nonlinearities—see Eq. (9)—are only functions of the c_j 's. This improves the accuracy of the constraint equations, as several higher order (error generating) effects are eliminated. Secondly, the nature of the nonlinearity results in nonlinear coefficients (such as σ and γ) which grow with the modal wave number. Therefore, nonlinear effects from higher linear modes are likely to be important for these systems. Nonlinearities which are "translational" (such as nonlinear springs between adjacent masses) do not share this property, and yield systems which approach linearity as the mode number is increased.

Results

Results are given for several cases. First, the time-dependent shape of the deformed beam is illustrated for motions occurring in the third nonlinear mode, and the relationship between modal amplitude and response frequency is discussed for the first three modes. Next, the rotation rate, Ω , is tuned to create a 3:1 internal resonance between the first two transverse modes. Results generated from the reduced, 2-DOF NNM models of this system are then compared to those of the reference model. Lastly, system parameters are adjusted to create an internal resonance between an axial mode and a transverse mode. As before, the proposed NNM approach is compared with other reduction methods.

One feature of the nonlinear normal mode method is that, although only one mode is simulated, the time behavior of the slaved linear modes can be reconstructed through the constraint equations. This results in nonlinear modes which change shape with amplitude and velocity, and hence also time (also known as nonsimilar NNM's [16]). This property is illustrated in Fig. 7, where the functions $w(x,t)$ and $u(x,t)$ are reconstructed from a simulation time-history and the relevant constraint equations. Mode shapes are shown for several instants of time, spaced evenly over a quarter-period of motion. The nonsimilar nature of $w(x,t)$ is not especially noticeable, although the peak displacement of the first lobe does move to the right as the amplitude decreases. Note that, for $u(x)$, the static solution is included (the dashed line), and that all departures from this solution are nonsimilar, as the axial and transverse motions are linearly uncoupled. Also, for $u(x,t)$, the shapes shown are representative of the entire periodic behavior. That is, while $w(x,t)$ would become symmetric about the

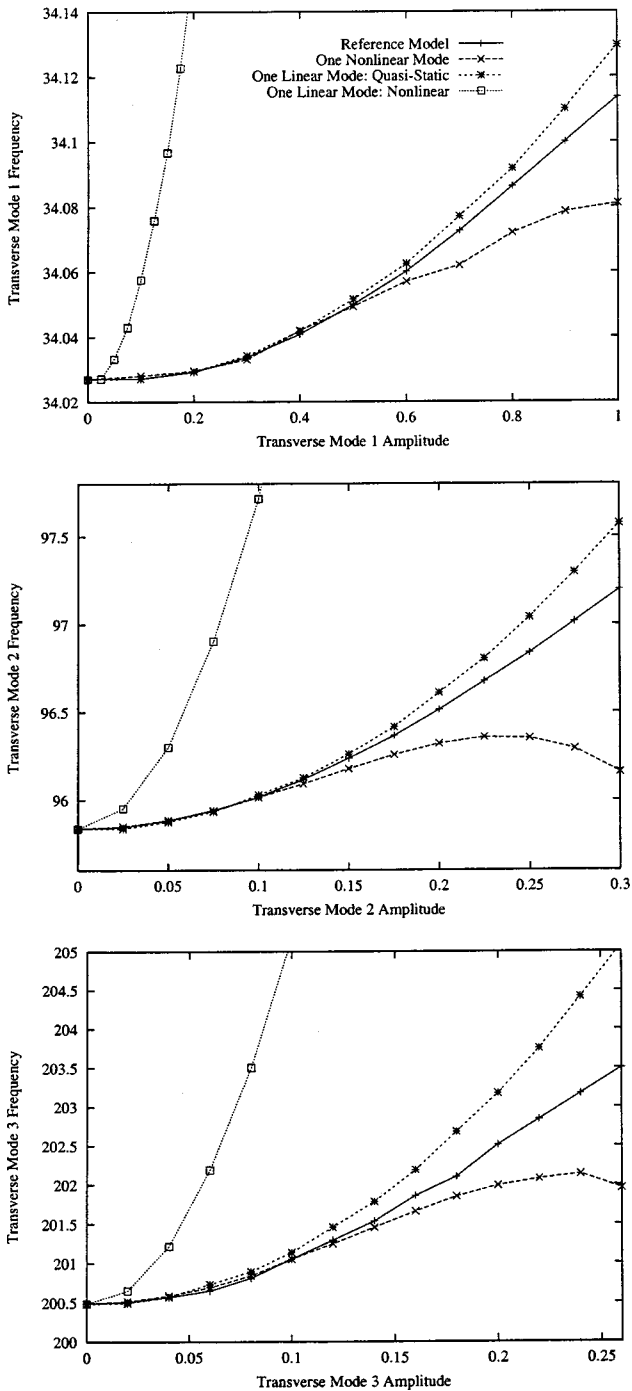


Fig. 8 Response frequency as a function of modal amplitude for several one-mode models, as well as the reference solution, for the first three transverse modes

x -axis with further time sampling, the corresponding axial motion, $u(x,t)$, would simply repeat over the range shown (at twice the frequency of $w(x,t)$).

Further insight may be obtained through examination of Fig. 8, which illustrates the relationships between the response frequencies and amplitudes for the first three nonlinear modes, using various models. Here, the “Reference Model” indicates the frequency of a periodic solution for the full 18-DOF model, found through numerical searching methods. This solution lies on the “exact” invariant manifold of the reference model, and is successfully approximated by our nonlinear mode approach over a range that is

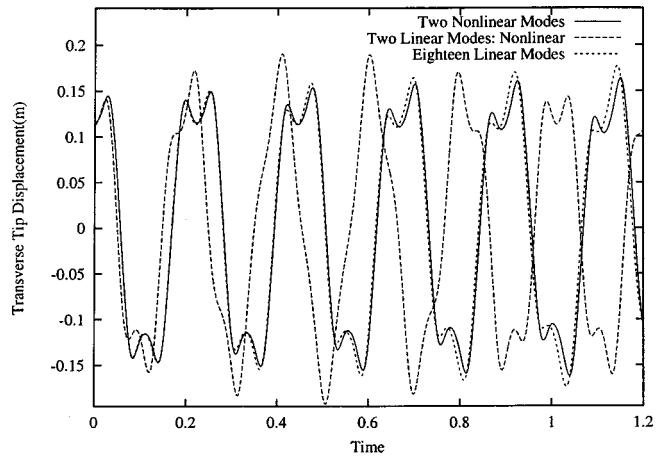


Fig. 9 Transverse deflection, $w(L,t)$, initiated on a two-mode (first and second transverse) nonlinear manifold with $3\omega_{t,1} \approx \omega_{t,2}$, for the reference (18-DOF) and various reduced (2-DOF) models

particular to each mode. The quasi-static results shown here illustrate the effects of eliminating axial independence through the quasi-static assumptions described previously. This approach relies on the distinct separation between the axial and transverse modes. While quite effective here, it is not readily extendible to realistic blade geometries, as the modes of these models do not fall so nicely into such distinct categories. The “One Linear Mode” result eliminates the influence of all other linear modes, that is, it is a projection of the equations of motion onto the corresponding linear mode, and consequently the results diverge quite quickly. The divergence observed between the nonlinear mode results and the reference solutions as the amplitude increases is due to large amplitude effects which are not captured by the third-order manifold employed here. Model fidelity could be improved through the inclusion of higher-order terms in the expansions for the invariant manifolds, and thus the generation of higher order terms in the NNM equations of motion. As an aid for physical interpretation of these results, a tip displacement of 0.2 m approximately corresponds to a transverse modal amplitude of 1.0 (for all transverse modes).

A 3:1 internal resonance between the first two transverse modes was created by adjusting the rotation rate, Ω , from 30 to 23.85 rad/s. Conditions such as this may easily occur during typical operations. As with the single-mode results above, Fig. 9 depicts results from various two-DOF reduced systems, and their comparison with the reference results. Here, the reference (Eighteen Linear Modes) model dynamics are initiated on the approximate invariant manifold. That is, the initial conditions in the mode(s) of interest are chosen, and then the remaining degrees of freedom are assigned their initial values according to the constraint equations, Eq. (14). For this case, the coupling between the two resonant modes is well captured by the nonlinear normal mode approach, which requires the calculation of a two-mode (four-dimensional) invariant manifold, and yields a fully coupled, two-DOF, reduced model. The “Two Linear Modes: Nonlinear” response is obtained by projecting the equations of motion directly onto the two linear, resonant modes. This model includes the nonlinear coupling between the modes, but fails to achieve the proper qualitative or quantitative results, due to the fact that other linear (slave) modes contribute to the more accurate results. Under these circumstances, the proposed reduction procedure is particularly attractive. The effectiveness of the manifold constraint equations for predicting the dynamics of nonmodeled modes can be observed in Fig. 10. Here the two curves shown depict the behavior of the slaved ninth linear transverse mode for the motion shown in Fig. 9. It compares the dynamics obtained through numerical integra-

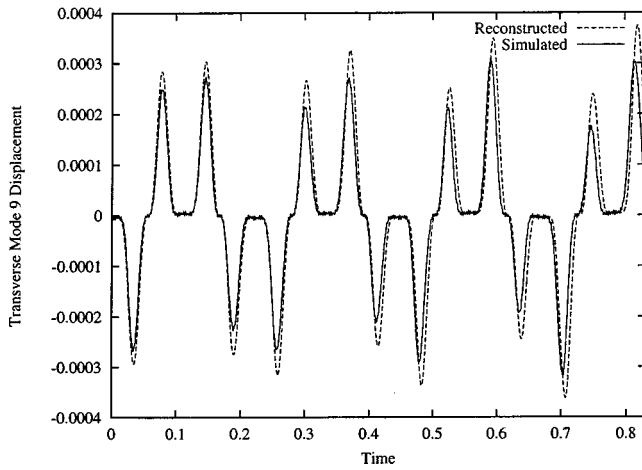


Fig. 10 Modal deflection of the ninth transverse mode, $c_9(t)$, initiated on a two-mode (first and second transverse) nonlinear manifold with $3\omega_{t,1} \approx \omega_{t,2}$ as predicted by simulation, and reconstructed using the constraint equations, Eq. (14)

tion of the entire system with those predicted by the manifold constraint equations. That is, the “Simulated” curve is a result of the dynamic interactions of a 18-DOF system, while the “Reconstructed” curve is a polynomial combination of the positions and velocities of the first and second transverse modes, based on the invariant manifold constraint equations. It is precisely this motion, and the other slave motions (not shown) which must occur for this two-mode response to be invariant.

Lastly, a 2:1 internal resonance between the first axial mode and the fourth transverse mode exists for following parameter values: $m = 11.84 \text{ kg/m}$, $EI = 4.73 \times 10^5 \text{ N m}^2$, $EA = 1.89 \times 10^8 \text{ N}$, $\Omega = 30 \text{ rad/s}$, and $h = 0 \text{ m}$. As before, the results in Fig. 11 show considerable error when the slaved linear modes are not accounted for. The “Two Linear Modes: Nonlinear” results, though internally resonant, exhibit a period of modulation which is entirely wrong. Of course, if more linear modes are simply added, these results will improve, but in cases such as this it is often difficult to deduce which additional linear modes would yield the most improvement. These questions are automatically resolved through

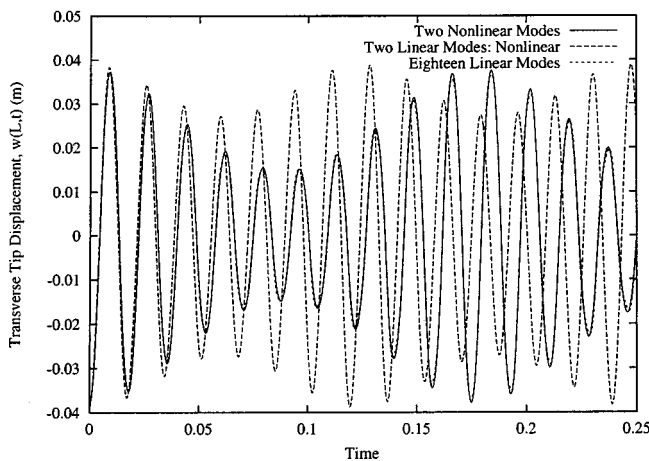


Fig. 11 Transverse deflection, $w(L,t)$, initiated on a two-mode (fourth transverse and first axial) nonlinear manifold with $2\omega_{t,4} \approx \omega_{a,1}$, for the reference (18-DOF) and various reduced (2-DOF) models

the use of invariant manifold-based nonlinear normal modes, since they systematically account for all other slaved modes, thus avoiding guesswork and oversized models.

Conclusions

The above results illustrate the utility of the invariant manifold-based approach for generating nonlinear normal modes. For the rotating beam system considered, there are critical nonlinear couplings between the system’s linear modes which must be accounted for if accurate results are to be obtained. Specifically, the coupling between the transverse and axial modes, due to bending-induced axial foreshortening effects, is essential. The NNM approach accurately estimates the influence of this coupling for moderate amplitude motions, generating minimal models which retain considerable accuracy.

In addition, the systematic nature of the reduction process makes it applicable to more complex blade models. In geometrically correct blade models, the system modes no longer occur in easily separable categories. Likewise, the nonlinearities do not share the ordered structure of the present model. However, if the linear modes are known, and the nonlinear coupling terms have been determined, the reduction process remains unchanged. Hence, the methods proposed herein may readily be extended to more realistic rotorcraft blade models, ultimately yielding optimal reduced models with minimal guesswork.

With this goal in mind, there are some particular issues which require further attention. The blade model must be shifted from analytical to finite-element based, allowing the generation of models with complex geometry and material properties. This generalization requires work at the element level, due to the nature of the nonlinearities involved, but will enable the inclusion of more general motions, such as torsion and lead-lag. Such work is underway [17]. In addition, recent work by the authors has provided a method for numerically solving the invariant manifold equations. Not only does this give the user control over the accuracy of the manifold solution, it significantly extends the amplitude range of the NNM-based models [18,19].

Acknowledgments

This work was supported by a grant from the U.S. Army Research Office. Dr. Gary Anderson is the grant monitor. The authors are grateful to Mr. Dongying Jiang for assistance with preparation of the manuscript.

References

- [1] Friedmann, P. P., 1977, “Recent Developments in Rotary-Wing Aeroelasticity,” *J. Aircr.*, **14**(11), pp. 1027–1041.
- [2] Hodges, D. H., Hopkins, A. S., and Kunz, D. L., 1989, “Analysis of Structures with Rotating, Flexible Substructures Applied to Rotorcraft Aeroelasticity,” *AIAA J.*, **27**(2), pp. 192–200.
- [3] Kosmatka, J. B., and Friedmann, P. P., 1989, “Vibration Analysis of Composite Turbopropellers Using a Nonlinear Beam-Type Finite-Element Approach,” *AIAA J.*, **27**(11), pp. 1606–1614.
- [4] Hodges, D. H., and Dowell, E. H., 1974, “Nonlinear Equations of Motion for the Elastic Bending and Torsion of Twisted Nonuniform Rotor Blades,” Technical Report TN D-7818, NASA.
- [5] Crespo Da Silva, M., and Hodges, D. H., 1986, “Nonlinear Flexure and Torsion of Rotating Beams, With Application to Helicopter Rotor Blades—I. Formulation,” *Vertica*, **10**(2), pp. 151–169.
- [6] Simo, J. C., and Vu-Quoc, L., 1988, “On the Dynamics in Space of Rods Undergoing Large Motions—A Geometrically Exact Approach,” *Comput. Methods Appl. Mech. Eng.*, **66**, pp. 125–161.
- [7] Wright, A. D., Smith, C. E., Thresher, R. W., and Wang, J. L. C., 1982, “Vibration Modes of Centrifugally Stiffened Beams,” *ASME J. Appl. Mech.*, **49**, pp. 197–202.
- [8] Du, H., Lim, M. K., and Liew, K. M., 1994, “A Power Series Solution for Vibration of a Rotating Timoshenko Beam,” *J. Sound Vib.*, **175**(4), pp. 505–523.
- [9] Naguleswaran, S., 1994, “Lateral Vibration of a Centrifugally Tensioned Uniform Euler-Bernoulli Beam,” *J. Sound Vib.*, **176**(5), pp. 613–624.
- [10] Yoo, H. H., and Shin, S. H., 1998, “Vibration Analysis of Rotating Cantilever Beams,” *J. Sound Vib.*, **212**(5), pp. 807–828.
- [11] Pesheck, E., Pierre, C., Shaw, S. W., and Boivin, N., 2001, “Nonlinear Modal

- Analysis of Structural Systems Using Multi-mode Invariant Manifolds,” *Nonlinear Dyn.*, in press.
- [12] Shaw, S. W., and Pierre, C., 1993, “Normal Modes for Non-Linear Vibratory Systems,” *J. Sound Vib.*, **164**(1), pp. 85–124.
- [13] Shaw, S. W., and Pierre, C., 1994, “Normal Modes of Vibration for Non-Linear Continuous Systems,” *J. Sound Vib.*, **169**(3), pp. 319–347.
- [14] Meirovitch, L., 1967, *Analytical Methods in Vibrations*, MacMillan Publishing Co., Inc.
- [15] Shaw, S. W., Pierre, C., and Pesheck, E., 1999, “Modal Analysis-Based Reduced-Order Models for Nonlinear Structures—An Invariant Manifold Approach,” *Shock Vib. Dig.*, **31**(1), pp. 3–16.
- [16] Vakakis, A. F., Manevitch, L. I., Mikhlin, Y. V., Pilipchuck, V. N., and Zevin, A. A., 1996, *Normal Modes and Localization in Nonlinear Systems*, John Wiley & Sons.
- [17] Apiwattanalungarn, P., Shaw, S. W., Pierre, C., and Jiang, D., 2001, “Finite-Element-Based Nonlinear Modal Reduction of a Rotating Blade with Large-Amplitude Motion,” *Nonlinear Dynamics*, to appear.
- [18] Pesheck, E., Pierre, C., and Shaw, S. W., 2001, “A New Galerkin-Based Approach for Accurate Nonlinear Normal Modes Through Invariant Manifolds,” *J. Sound Vib.*, in press.
- [19] Pesheck, E., Pierre, C., and Shaw, S. W., 2001, “Accurate Reduced-Order Models for a Simple Rotor Blade Model Using Nonlinear Normal Modes,” *Math. Comput. Modell.*, **33**, pp. 1085–1097.